Available online at www.sciencedirect.com
ScienceDirect
Ceramics International 34 (2008) 225–229
CERAMICS INTERNATIONAL
www.elsevier.com/locate/ceramint

Preparation and electrochemical behavior of sol–gel $LiNi_{0.3}Co_{0.70-x}M_xO_2$ (M = Mn, Al)

Aracely Hernández *, Silvia Fabela, Luis Carlos Torres-González, Eduardo Sánchez

Facultad de Ciencias Químicas, Universidad Autónoma de Nuevo León, Pedro de Alba s/n, Cd. Universitaria, San Nicolás de los Garza Nuevo León, Mexico

Received 15 June 2006; received in revised form 4 July 2006; accepted 8 September 2006
Available online 13 November 2006

Abstract

$LiNi_{0.3}Co_{0.70-x}M_xO_2$ (M = Mn, Al) powders were synthesized using as a precursor, an aqueous or alcoholic mixture of metal organic salts with citric acid as chelating agent. Resulting powders were characterized by thermal analysis (TGA–DTA), X-ray diffraction (XRD), infrared spectroscopy (FT-IR) and scanning electron microscopy (SEM). Desired crystalline structure was developed at 700 °C. $LiNi_{0.3}Co_{0.7}O_2$ powders exhibit a layered α-$NaFeO_2$ structure (space group: $R\bar{3}m$). Electrochemical characteristics of the synthesized materials were evaluated on Swagelock^{TM} cells on a Li/$LiNi_{0.3}Co_{0.70-x}M_xO_2$ configuration. For $LiNi_{0.3}Co_{0.7}O_2$ the initial capacity was 142 ± 5 mAh/g and for $LiNi_{0.3}Co_{0.6}Mn_{0.1}O_2$ similar capacity was exhibited. On the other hand, a decrease on cell capacity was observed when Co substitution was done with aluminum.

Keywords: Lithium–nickel–cobalt oxide; Sol–gel citrate method; XRD

1. Introduction

Manufacture of rechargeable lithium batteries represents a major industrial activity. Layered lithiated transition metal oxides are of great interest as positive electrode materials. Although $LiCoO_2$ with hexagonal α-$NaFeO_2$ structure has been commercialized, development of future rechargeable lithium ion batteries is dependent on replacing this electrode to enhance its stability and specific capacity. Li_2MnO_4 and $LiNiO_2$ have been extensively investigated [1–4]. $LiNiO_2$ is hard to synthesize and is unstable due to its phase transitions and nonstoichiometry. The practical problem that prevents Li_2MnO_4 from reaching the commercial stage is its reduced capacity as the number of cycles is increased [5]. Many research groups have focused on synthesizing new lithium transition metal oxides which can fulfill the requirements as positive electrode material, with the advantage of being less toxic than $LiCoO_2$ combined with a higher capacity to cycle lithium ($LiCoO_2$ exhibits a capacity of 130 mAh/g) [6].

The layered compound $LiNi_{1-x}Co_xO_2$, is a promising cathode material for lithium ion secondary batteries since lithium–nickel–cobalt mixed oxides provide high specific capacity and good cycling stability. However, structural instability compared with $LiCoO_2$ was recently reported [7]. Some researchers have pointed out that partial substitution of Co enhances the structural stability of layered $LiNi_{1-x}Co_xO_2$ and many attempts for searching new substitutes have been made [8]. Among these potential substitutes manganese has been used due to its high average redox potential [9]. On the other hand, improvement of retention capacity of $LiMn_2O_4$ has been achieved when some trivalent or divalent cations were used on partial substitution of manganese ions [10]. It has been reported for lithium nickel mixed oxides, that thermal stability in the charged state and cyclability can be enhanced by aluminum [11].

The classical ceramic method for preparing materials does not ensure a high level of homogeneity in the final composition. In recent years various low-temperature preparation techniques, such as sol–gel, precipitation, hydrothermal and combustion synthesis have been developed [12,13]. The alkoxide sol–gel route is widely accepted for synthesizing advanced materials with tailored properties. However, for

* Corresponding author. Tel.: +52 81 83294010x6363; fax: +52 81 83765375.
E-mail address: ahernandez@fcq.uanl.mx (A. Hernández).

0272-8842/$32.00
doi:10.1016/j.ceramint.2006.09.010

large-scale application it is somehow expensive; therefore, several alternative methods have been developed, for example, the inexpensive ''inorganic sol–gel'' route, consisting on an aqueous or alcoholic mixture of metal organic salts with a chelating agent such as citric acid, called sol–gel citrate method. The main advantage of the sol–gel method is the molecular level homogeneous mixing of transition-metal cation which enhances the formation of polycrystalline particle with improved electrochemical properties [14].

In this paper, we propose the synthesis by the sol–gel citrate method of the layered compound $LiNi_{0.3}Co_{0.70-x}M_xO_2$ where M = Mn or Al, in order to study the effect of Co substitution on its thermal, textural and electrochemical characteristics.

2. Experimental

2.1. Synthesis

We used $LiCH_3CO_2{\cdot}2H_2O$, $Ni(CH_3CO_2)_2{\cdot}4H_2O$, $Co(CH_3CO_2)_2{\cdot}4H_2O$, $Mn(CH_3CO_2)_2{\cdot}4H_2O$ and $Al(CH_3CO_2)_3{\cdot}4H_2O$ to prepare $LiNi_{0.3}Co_{0.70-x}M_xO_2$ (M = Mn, Al). Metallic acetates (2.5–3.0 g), were poured inside an aluminum pan and then 12–15 mL of 1.0 M citric acid $HOC(CO_2H)(CH_2CO_2H)_2$ solution was carefully added and mixed for about 30 min. In some cases 5–15 mL of deionized water were added to complete dissolution. The solution was slowly warm up to 80 °C for a period of 24–48 h to evaporate most of the water until a jelly-like residue was formed. Afterwards, the gel precursor was transferred to a platinum crucible and calcined at 400–700 °C for 6–24 h; dark powders were obtained.

2.2. Characterization

Thermal analysis on the precursor complex (gel or paste) was performed using a simultaneous DTA/TGA equipment (TA Instruments model SDT-2960) from room temperature up to 800 °C. Thermograms were obtained using a steady flow of dry air of 100 mL/min and a typical heating rate of 10 °C/min. The infrared IR spectra of samples from the different temperatures were recorded in a FT-IR Perkin-Elmer Paragon 1000 PC spectrophotometer working in a 4000–400 cm^{-1} frequency range using KBr pellets.

X-ray diffraction patterns were obtained with a Siemens D5000 X-ray diffractometer using a nickel-filtered Cu Kα λ = 1.5418 Å source. Difractograms were taken between 10° and 90° using a step size of 0.1 degrees at a scan rate of 2.3°/min for structure evolution experiments and between 10° and 80° using a step size of 0.1° at a scan rate of 0.1°/min for structure confirmation.

In order to confirm the chemical composition of the different lithiated transition metal oxides prepared by sol–gel, we carried out atomic absorption spectroscopy studies (AA spectrophotometer Zhimadzu 6650). Scanning electronic microscopy (SEM: LEICA S-440) was used to observe the morphology of the synthesized materials.

2.3. Electrochemical experiments

Electrochemical experiments were carried out in a multichannel potentiostatic–galvanostatic MacPile II system [15], using a Swagelock™ type cell [16]. Electrochemical cells were constructed using a two electrode configuration where metallic lithium was used as negative electrode. Layered cathode was a 7 mm diameter pellet, prepared by mixing-up 20 mg of low-temperature synthesized dark powder with electrolytic black carbon and EPDT (ethylene–propylene–diene terpolymer in ciclohexane at 0.5% (v/v)), acting as a binder on a 79:20:1 ratio. Battery grade electrolyte, a 1.0 M $LiClO_4$ solution on a freshly distilled 1:1 ethylene and propylene carbonate mixture was used. The charge/discharge experiments were carried out between 2.2 and 4.2 V potential ranges at a current density of 0.1 mA/cm^2.

3. Results and discussion

3.1. Chemical analysis

Table 1 shows the chemical composition according to atomic absorption spectroscopy studies. As chemical composition obtained is very close to target, it was confirmed that the sol–gel citrate method is an appropriate synthetic route to avoid metal losses, especially lithium losses, that occurred when the solid-state method is used in the synthesis of mixed oxides.

3.2. Thermal analysis

The TGA/DTA curve of gel precursor for $LiNi_{0.3}Co_{0.6}Mn_{0.1}O_2$ is shown in Fig. 1. The initial weight loss of 5% from room temperature to 220 °C was caused by removal of physically absorbed water. The main weight loss of 33% between 230 and 335 °C is attributed to the decomposition of

Table 1
Chemical composition for different electrode materials $LiNi_{0.3}Co_{0.7-x}M_xO_2$ (M = Mn, Al) sol–gel

Material	Expected *X*	Li (%P)	Ni (%P)	Co (%P)	Mn (%P)	Al (%P)	Obtained *X*
$LiNi_{0.3}Co_{0.7}O_2$	0	7.06	15.93	41.90	–	–	0
$LiNi_{0.3}Co_{0.6}Mn_{0.1}O_2$	0.1	6.94	16.28	36.00	5.63	–	0.1
$LiNi_{0.3}Co_{0.5}Mn_{0.2}O_2$	0.2	6.85	16.14	31.22	12.36	–	0.22
$LiNi_{0.3}Co_{0.4}Mn_{0.3}O_2$	0.3	7.11	17.10	24.36	17.90	–	0.31
$LiNi_{0.29}Co_{0.6}Al_{0.1}O_2$	0.1	6.82	17.39	35.82	–	2.70	0.1
$LiNi_{0.3}Co_{0.5}Al_{0.2}O_2$	0.2	7.26	18.0	32.0	–	5.35	0.20
$LiNi_{0.29}Co_{0.4}Al_{0.3}O_2$	0.3	7.27	16.85	26.72	–	8.31	0.31

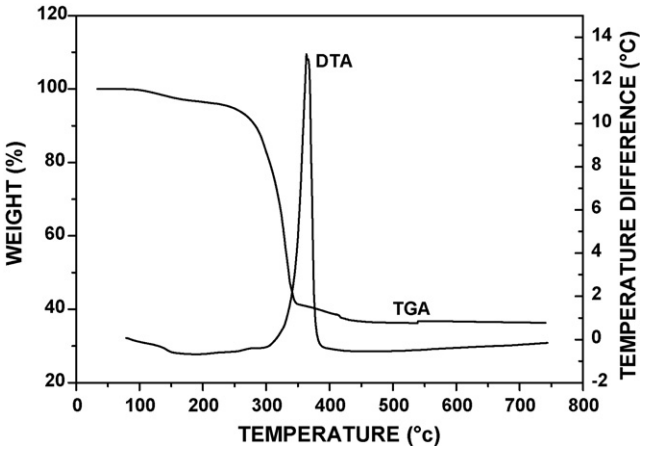

Fig. 1. DTA and TGA curves of $LiNi_{0.3}Co_{0.6}Mn_{0.1}O_2$ fresh sample.

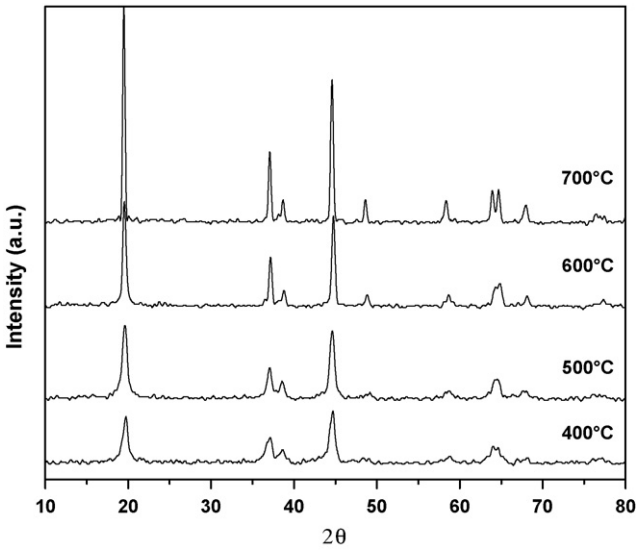

Fig. 2. XRD patterns of gel evolution of $LiNi_{0.3}Co_{0.7}O_2$ with temperature.

citrate and residual acetate groups. The last weight loss from 336 to 430 °C is due to the dehydroxylation process since retention of hydroxyl groups, even at relatively high temperatures, is a typical behavior of most solids prepared by a sol–gel process. This is in agreement with the vanishing of the corresponding O–H bands in the FT-IR spectra. A large exothermic peak at 336 °C can be observed in the DTA curve which corresponds to decomposition and oxidation of organic precursors [17]. Similar curves were obtained for different compositions of prepared $LiNi_{0.3}Co_{0.7-x}M_xO_2$ (M = Mn, Al).

3.3. X-ray diffraction

Fig. 2 shows X-ray diffraction patterns of the gel evolution of $LiNi_{0.3}Co_{0.70}O_2$ with temperature. When the powder is heated from 400 to 600 °C some peaks are observed, which is indicative of a crystalline structure evolution. Once the fresh sample is heated at 700 °C, the xerogel is transformed into a crystalline material with a powder pattern similar to that reported for α-$NaFeO_2$ structure (space group: $R\bar{3}m$). The XRD spectra at 700 °C, shows a single phase of layered structure with a good crystallinity. Previous works [18] indicate that materials prepared by the sol–gel citrate method exhibit a better crystallinity than those synthesized by solid-state reaction where precursors mixture is heated at 1000 °C for 48 h, moreover, the sol–gel method allows to obtain layered compound at low temperature and less heating time, which represents a significant energy saving.

The X-ray powder diffraction patterns of the $LiNi_{0.3}Co_{0.7-x}Mn_xO_2$ ($x = 0.1$, 0.2, 0.3) are shown in Fig. 3a. The crystalline structure of the samples was also obtained at 700 °C. We can see that the most important reflections of α-$NaFeO_2$ structure are matched for all samples and a high degree of crystallinity is present, indicated by the quite narrow peaks. The Co substitution by manganese does not cause important

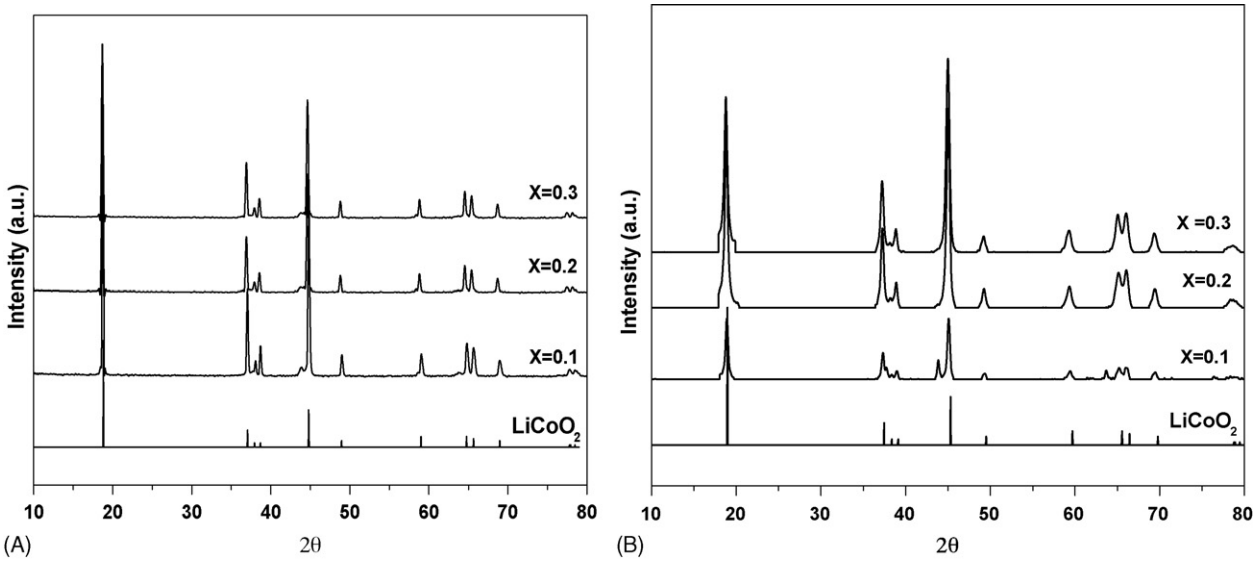

Fig. 3. XRD patterns of (a) $LiNi_{0.3}Co_{0.7-x}Mn_xO_2$ and (b) $LiNi_{0.3}Co_{0.7-x}Al_xO_2$ ($x = 0$, 0.1, 0.2 and 0.3).

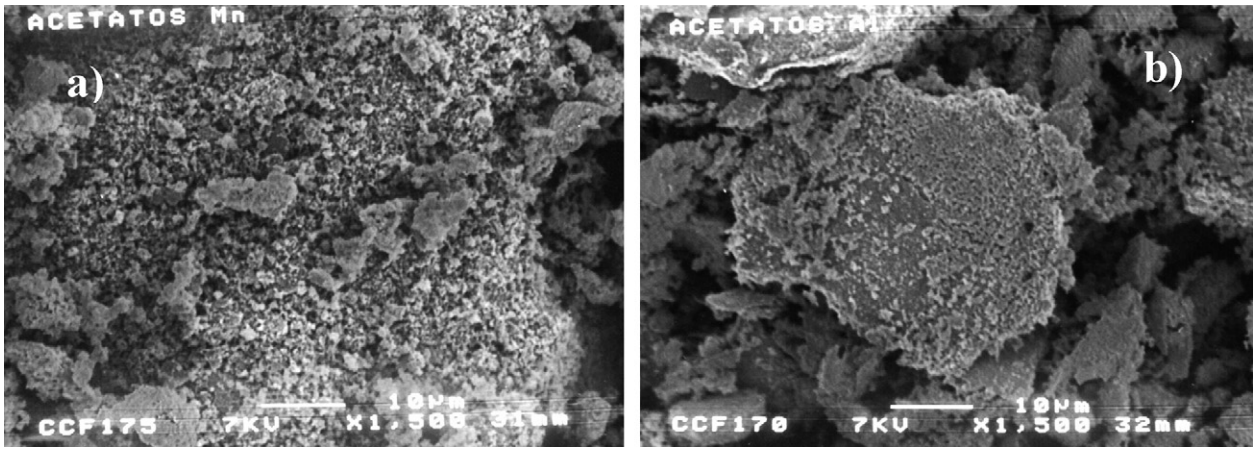

Fig. 4. SEM images of (a) $LiNi_{0.3}Co_{0.4}Mn_{0.3}O_2$ and (b) $LiNi_{0.3}Co_{0.6}Al_{0.1x}O_2$. The scale bar is 10 μm long.

changes in lattice arrangement. Another research group [19], also reported that manganese is uniformly mixed on the transition-metal sites when forming a mixed transition-metal material as a possible replacement for $LiCoO_2$; this novel layered compounds are solid solution phases.

On the other hand, the XRD patterns of samples where Co substitution was done by ion aluminum(III) are shown in Fig. 3b. XRD diagrams show broad and poorly defined peaks suggesting low crystallinity. Reflections on $LiNi_{0.3}Co_{0.7-x}Al_xO_2$ ($x = 0.1$) show a peak at 44° θ angle due to impurity phase. As the content of Al increases from $x = 0.2$ to 0.3 a structure deformation is observed, mainly indicated by reflection $2\theta = 19°$.

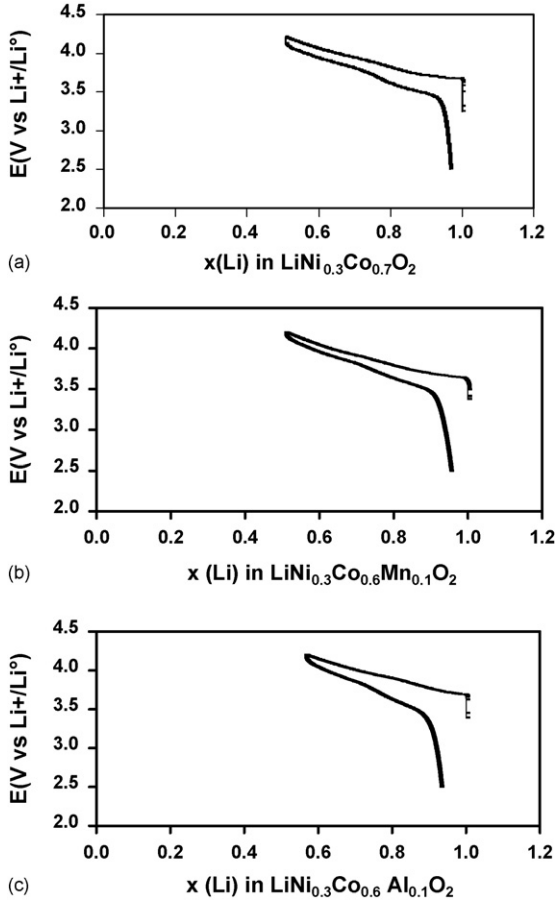

Fig. 5. Evolution of cell voltage for experiments run in cells configured as: (a) Li//$LiNi_{0.3}Co_{0.7}O_2$, (b) Li//$LiNi_{0.3}Co_{0.6}Mn_{0.1}O_2$, and (c) Li//$LiNi_{0.3}Co_{0.6}Al_{0.1}O_2$.

3.4. Morphologies of the synthesized materials

SEM images are shown in Fig. 4 for $LiNi_{0.3}Co_{0.4}Mn_{0.3}O_2$ and $LiNi_{0.3}Co_{0.6}Al_{0.1}O_2$ samples. Similar micrographs were obtained for all the other synthesized samples having a non-regular distribution of particle size. SEM micrograph of manganese layered oxide shows small primary particles with diameter ranging between 300 and 500 nm which tend to form aggregates of approximately 5–12 μm diameter size. Particle morphology of $LiNi_{0.3}Co_{0.7-x}Al_xO_2$ samples (Fig. 4b) exhibits a large number of secondary particles having a distribution of 20–50 μm. The secondary particles consist of primary particles with a size diameter <1 μm.

3.5. Electrochemical behavior

Fig. 5 shows the evolution of cell voltage with composition, for experiments run in cells configured as: Li//$LiNi_{0.3}Co_{0.7}O_2$, Li//$LiNi_{0.3}Co_{0.6}Mn_{0.1}O_2$, and Li//$LiNi_{0.3}Co_{0.6}Al_{0.1}O_2$, respectively. From their curves we can observe similar initial charge/discharge profiles. The shape of the cycling curve is characteristic of one phase domain and no structural changes are present at potentials between 2.2 and 4.2 V. Similar curves were obtained for different compositions of prepared $LiNi_{0.3}Co_{0.7-x}M_xO_2$ (M = Mn, Al) for $x = 0.2$ and 0.3.

Table 2 shows specific capacity (mAh/g) and the intercalated–deintercalated lithium for each composition calculated from electrochemical experiments. From these results, we can observe for $LiNi_{0.3}Co_{0.6}Mn_{0.1}O_2$ the same capacity as for $LiNi_{0.3}Co_{0.7}O_2$, however, as the manganese content is increasing, the capacity is somehow decreasing. This behavior may be due to increase in Co^{4+} content and the corresponding decrease in Co^{3+}. It was reported [20] that in cobalt-substituted

Table 2
Calculated specific capacity (mAh/g) for $LiNi_{0.3}Co_{0.7-x}M_xO_2$ (M = Mn, Al)

Material	Capacity (mAh/g)	Deintercalated lithium
$LiNi_{0.3}Co_{0.7}O_2$	142.4	0.52
$LiNi_{0.3}Co_{0.6}Mn_{0.1}O_2$	142.3	0.51
$LiNi_{0.3}Co_{0.5}Mn_{0.2}O_2$	127.0	0.46
$LiNi_{0.3}Co_{0.4}Mn_{0.3}O_2$	103.0	0.42
$LiNi_{0.3}Co_{0.6}Al_{0.1}O_2$	137.4	0.51
$LiNi_{0.3}Co_{0.5}Al_{0.2}O_2$	98.0	0.35
$LiNi_{0.3}Co_{0.4}Al_{0.3}O_2$	–	–

phases is easier to oxidize nickel than cobalt to the tetravalent state.

When Co substitution with aluminum was done, the cell capacity decreases. The low crystallinity grade exhibited in the XRD patterns for this material affect the charge/discharge specific capacity, in agreement with the usually observed behavior for lower crystalline electrode materials [11].

On the other hand, it is known that capacity depends on the vacancy content and replacing ion concentration, when the valence of the cation is constant. Then, it could be possible decrease capacity to be due to the presence of constant valent Al^{3+} ions, which force electron exchange with oxygen during topotatic reaction. This agrees with the theoretical capacity of trivalent-ion-doped $LiCoO_2$ calculated for various values of vacancy concentration by Venkatraman et al. [5], who predicts a decrease in capacity with increased aluminum concentration.

4. Conclusions

We have successfully synthesized a layered $LiNi_{0.3}Co_{0.70-x}M_xO_2$ (M = Mn, Al) by the sol–gel citrate method. The crystalline phase was obtained at lower temperature (700 °C) than for the solid-state method. For composition containing manganese, we obtain a homogeneous material with a higher crystalline grade than for composition containing aluminum. The electrochemical behavior of manganese material shows a good practical specific capacity of 142 mAh/g when $x = 0.1$, superior to that reported for $LiCoO_2$. When we synthesize the lithiated transition metal oxides with aluminum, we found that trivalent cation causes a decrease on cell capacity when used as cathode in a $Li/LiNi_{0.3}Co_{0.70-x}Al_xO_2$.

Acknowledgements

The authors gratefully acknowledge financial support of SEP under grant PROMEP/103.5/03/2553, UANL under grant PAICYT CA848-04 and CA851-04 and NSF-CONACYT under grant no. 35998U. We are grateful to Carlos Amador for technical assistance in SEM technique.

References

[1] D. Larcher, M.R. Palacin, G.G. Amatucci, J.M. Tarascon, Electrochemically active $LiCoO_2$ and $LiNiO_2$ made by cationic exchange under hydrothermal conditions, J. Electrochem. Soc. 144 (1997) 408.
[2] H. Arai, S. Okada, Y. Sakurai, J. Yamaki, Electrochemical and thermal behavior of $LiNi_{1-z}M_zO_2$ (M = Co, Mn, Ti), J. Electrochem. Soc. 144 (1997) 3117.
[3] M.M. Rao, M. Jayalaskshmi, O. Schaf, H. Wulff, U. Guth, F. Scholz, Electrochemical behaviour of solid lithium cobaltate ($LiCo_2$) and lithium manganate ($LiMn_2O_4$) in an aqueous electrolyte system, J. Solid State Electrochem. (2001) 50.
[4] Y.J. Wei, L.Y. Yan, C.Z. Wang, X.G. Xu, F. Wu, G. Chen, Effects of Ni doping on $[MnO_6]$ octahedron in $LiMn_2O_4$, J. Phys. Chem. B 108 (2004) 18547.
[5] S. Venkatram, V. Subramanian, S. Gopu Kumar, N.G. Renganathan, N. Muniyandi, Capacity of layered cathode materials for lithium-ion batteries—a theoretical study and experimental evaluation, Electrochem. Commun. 2 (2000) 18.
[6] P.G. Bruce, A.R. Armstrong, R.L. Gitzendanner, New intercalation compounds for lithium batteries: layered $LiMn_2O_4$, J. Mater. Chem. 9 (1999) 193.
[7] R.V. Chebiam, F. Prado, A. Manthiram, Comparision of the chemical stability of $Li_{1-x}Ni_{0.85}Co_{.15}O_2$ cathodes, J. Solid State Chem. 163 (2002) 5.
[8] P.-Y. Liao, J.-G. Duh, Synthesis and characterization of $LiNi_xCo_yMn_{1-x-y}O_2$ as a cathode material for lithium ion batteries, Trans Tech Publications, Eng. Mater. 280–283 (2005) 677.
[9] Q. Feng, Y. Xu, K. Kajiyoshi, K. Yanagisawa, Hydrothermal soft chemical synthesis of $Ni(OH)_2$-birnessite sandwich layered compound and layered $LiNi_{1/3}Mn_{2/3}O_2$, Chem. Lett. (2001) 1036.
[10] M. Wohlfahrt-Mehrens, C. Vogler, J. Garche, Aging mechanisms of lithium cathode materials, J. Power Sources 127 (2004) 58.
[11] S. Albrechet, J. Kumpers, M. Kruft, S. Malcus, C. Vogler, M. Wahl, M. Wohlfhart-Mehrens, Electrochemical and thermal behavior of aluminum- and magnesium-doped spherical lithium nickel cobalt mixed oxides $Li_{1-x}(Ni_{1-y-z}Co_yM_z)O_2$ (M = Al, Mg), J. Power Sources 119–121 (2003) 178.
[12] S.R.S. Prabaharan, S.S. Michel, C. Julien, Synthesis, Electrochemistry of $LiMn_2O_4$ prepared using succinic acid as complexing agent, Int. J. Inorg. Mater. 1 (1999) 21.
[13] S.-T. Myung, M.-H. Lee, S.-H. Park, Y.-K. Sun, Hydrothermal synthesis of layered $Li[Ni_{0.5}Mn_{0.5}]O_2$ as lithium intercalation material, Chem. Lett. 33 (2004) 818.
[14] X. Li, F. Kang, W. Shen, X. Shi, Synthesis, Charge–discharge characteristics of polycrystalline $LiNi_{1-x}Co_xO_2$ ($0 < x < 0.5$) as a cathode material for lithium rechargeable batteries, Trans Tech Publications, Eng. Mater. 280–283 (2005) 443.
[15] C. Mouget, Y. Chabre, Multichannel potentiostat galvanostat Mac Pile. Licenced from CNRS and UJF Grenoble to Bio-Logic Corp., Claix, France.
[16] J.M. Tarascon, A new solid-state electrode for secondary lithium batteries, J. Electrochem. Soc. 132 (1985) 2089.
[17] M.K. Cinibulk, Synthesis of yttrium aluminum Garnet from a mixed-metal citrate precursor, J. Am. Ceram. Soc. 83 (5) (2000) 1276.
[18] S.H. Chang, S.-G. Kang, K.H. Jang, Electrochemical properties of $Li_xCo_yNi_{1-y}O_2$ prepared by citrate sol–gel method, Bull. Korean Chem. Soc. 18 (1997) 61.
[19] Z. Lu, Z. Chen, J.R. Dahn, Lack of cation clustering in $Li[Ni_xLi_{1/3-2x/3}Mn_{2/3-x/3}]O_2$ ($0 < x < 1/2$) and $Li[Cr_xLi_{(1-x)/3}Mn_{(2-2x)/3}]O_2$ ($0 < x < 1$), Chem. Mater. 15 (2003) 3214.
[20] C. Delmas, M. Menétrier, L. Croguennec, S. Levasseur, J.P. Pérés, C. Pouillerie, G. Prado, L. Fournés, F. Weill, Lithium batteries: a new tool in solid state chemistry, J. Inorg. Mater. 1 (1999) 11.